



**SINTEF**

# Report

## Geomagnetic induced currents in long subsea power cables

**Author(s):**

Kristian Solheim Thinn and Magnar Gullikstad Johnsen (UiT Norges Arktiske Universitet)

**Report No:**

2022:00759 - Unrestricted

**Client:**

Equinor Energy AS

# Report

## Geomagnetic induced currents in long subsea power cables

**KEYWORDS**

Geomagnetically induced currents  
GIC  
Long power cables  
Offshore  
Geomagnetic fields  
Space weather  
Solar storms  
Geomagnetic storms  
Power Grid

**VERSION**

1.0

**DATE**

2022-09-16

**AUTHOR(S)**

Kristian Solheim Thinn and Magnar Gullikstad Johnsen (UiT Norges Arktiske Universitet)

**CLIENT(S)**

Equinor Energy AS

**CLIENT'S REFERENCE**Jarle Bremnes  
PO: 4504080106**PROJECT NO.**

502003290

**NO. OF PAGES**

28

**EXECUTIVE SUMMARY**

This report focuses on geomagnetically induced currents (GIC) that can be induced in long subsea power cables. Literature indicates that the water depth itself, in which the cable will be laid, will not contribute to an attenuation of the geoelectric field for those water depths relevant for the Krafla power cable. However, the presence of a coast will introduce a strong enhancement.

Even minor (<20 years) and moderate (~20-100 years) geomagnetic events can potentially cause considerable operational difficulty if sufficient mitigations are not in place. A close cooperation with Statnett (transmission system operator) is essential to limit any unintentional disconnection of the Krafla subsea cable.

**PREPARED BY**

Kristian Solheim Thinn

SIGNATURE

  
Kristian Solheim Thinn  
Kristian Solheim Thinn (Sep 15, 2022 14:17 GMT+2)**CHECKED BY**


Olve Mo

SIGNATURE

  
Olve Mo  
Olve Mo (Sep 15, 2022 14:28 GMT+2)**APPROVED BY**

Dag Eirik Nordgård

SIGNATURE

  
Dag Eirik Nordgård  
Dag Eirik Nordgård (Sep 15, 2022 14:30 GMT+2)**REPORT NO.**

2022:00759

**ISBN**

978-82-14-07588-5

**CLASSIFICATION**

Unrestricted

**CLASSIFICATION THIS PAGE**

Unrestricted

# Document history

---

VERSION	DATE	VERSION DESCRIPTION
Draft	2022-08-10	Issued for information.
1.0	2022-09-16	Issued to Client.

---

# Table of contents

<b>1</b>	<b>SUMMARY AND CONCLUSIONS.....</b>	<b>4</b>
<b>2</b>	<b>INTRODUCTION.....</b>	<b>7</b>
<b>3</b>	<b>SOLAR STORMS AND HOW THEY AFFECT THE POWER GRID.....</b>	<b>8</b>
3.1	Introduction.....	8
3.1.1	GIC classification.....	8
3.1.2	From space weather to GIC.....	8
3.2	Consequences of GIC.....	9
3.3	Examples of historical GIC-events.....	10
3.3.1	Norway.....	10
3.3.2	Canada/US.....	10
3.3.3	Sweden.....	10
3.3.4	UK.....	10
3.4	Mitigate consequences of GIC.....	11
3.5	GIC and breakers.....	11
3.6	GIC and transformers.....	12
3.6.1	Standards.....	12
3.6.2	Full scale measurements.....	12
3.6.3	Design.....	13
3.6.4	Specifications in Sweden, Finland and Norway.....	13
3.7	Power system modelling of GIC.....	14
3.8	Measure GIC and correlate GIC to space weather measurements.....	14
3.8.1	Vendors.....	14
3.8.2	Measurement set-up.....	15
3.8.3	Measurements in Norway.....	15
3.9	Magnitude of B- and E-fields.....	15
<b>4</b>	<b>SEAWATER AND E-FIELD.....</b>	<b>17</b>
4.1	Depth effect.....	17
4.2	E-field of Krafla.....	19
4.3	Coastal effect.....	21
4.4	Summary.....	22
<b>5</b>	<b>GIC ESTIMATES FOR KRAFLA.....</b>	<b>23</b>
5.1	Introduction.....	23
5.2	Electrical circuit.....	23
5.3	GIC calculation.....	24
5.4	Reactive power consumption.....	24
	<b>REFERENCES.....</b>	<b>26</b>

# 1 SUMMARY AND CONCLUSIONS

## Introduction:

Geomagnetically induced currents (GIC) are produced by a naturally induced geoelectric field during geomagnetic disturbances. Phenomena from the Sun, such as Coronal Mass Ejections and Corotating Interaction Regions are strong transients in the solar wind that give rise to intensified space weather. In the event of such transients interacting with Earth's magnetic field, so called Geomagnetic Storms occur. During geomagnetic storms the current flowing within the magnetosphere-ionosphere system is enhanced, thus giving rise to larger than normal geomagnetic disturbances on ground. These enhanced geomagnetic disturbances are the cause of GICs. GIC is not a threat to the power cables themselves, but can become an problem if the transformers at each end of the cable have solid bonded (grounded) neutrals.

## Consequences and mitigations:

There are many good publications focusing on GIC: how GIC affects the power system, mitigations, historical GIC-events and lessons learned from these and how to perform detailed thermal modelling of transformers and the power grid during GIC events. The available literature is mainly directed towards transmission system operators (TSOs). A close cooperation with Statnett (Norwegian TSO) is essential to limit any unintentional disconnection of the Krafla subsea cable.

The main effects of GIC that have proven to give the largest consequences are

- Saturation of transformers in the transmission grid
- Increased reactive currents in the transmission grid, due to saturation of transformers
- Tripping of reactive compensation due to large harmonic currents, due to saturation of transformers.
- Shortage of reactive power, due to disconnection of compensation and increased reactive consumption by transformers
- Trip of transformer differential protection relays
- Disconnection due to overload on transmission lines due to high reactive power consumption
- Escalating situation with increased overloading, disconnections and stability issues, distortion, and worst-case full blackout.

In general, consequences of solar storms can be reduced by making the power grid more resistant to the effects of GIC, or by limiting the GIC that is induced by the solar storms:

- Install components blocking or reducing GIC (resistors, inductors, capacitors).
- Operate the power grid such that the amplitude of GIC is limited
- Operate the grid during solar storms with sufficient safety margins with regards to surplus active and reactive power. The grid can then handle the increase of reactive power consumption and possible disconnections without cascading disconnections, such as overload.
- Install transformers capable of handling larger DC currents with less saturation so that harmonics and increased reactive power is reduced
- Ensure that the transformers can manage increased losses as a consequence of GIC without excessive thermal overloading.
- Ensure that all relays are correctly coordinated so that there is no unintended (cascading) disconnection as a result of increased harmonics and increased reactive power consumption.

- Operate and dimension the grid so that the components (e.g. capacitor banks) are not as easily overloaded with high contents of harmonics.
- Ensure that atmospheric disturbance is considered in design of control systems and critical components.
- Operate the grid with temporary reduced loading on critical components during solar storms to avoid disconnections.
- Ensure that nominal current (peak value) of circuit breakers is less than the expected GIC.

**Circuit breakers:**

Current can only be interrupted when it becomes zero (or close to zero) during a 50/60 Hz cycle. Even for an extreme GIC event, there will be (based on estimated in this report) zero-crossing in the transformer circuit breaker current if Krafla is operated at more than 35% of nominal load. The load current through the reactor is normally smaller than in the transformer. Depending on the magnitude of GIC through this component (not estimated in this report), the topic may be more relevant for the reactor breaker. An evaluation of the probability of large GIC and the following consequences could be performed.

**Transformer specification:**

A three-legged three-phase transformer is more susceptible to GIC than a five-legged with respect to reactive effect consumption. One-phase transformers are more vulnerable. In Sweden (and from hearsay in Norway), transformers are specified to endure 100-200 A GIC for 10-15 minutes without thermal overloading.

**Measure GIC:**

An essential part of a GIC flow mitigation program is to install monitors to measure GIC flow and harmonics on a continuous basis. Monitors are a key source of real-time information that can guide system operators in determining real-time response. GIC can be measured on-line by commercially available clamp-on GIC-sensors, which are hall effect sensors with low-pass filter.

**Seawater and e-field:**

The North Sea and fjords themselves, with fairly modest depths of < 600 m and an average of ~100 m, will not contribute to any significant attenuation of the surface geoelectric field. However, the presence of the coast with a fairly shallow continental shelf which reaches far out (> 500 km), will introduce a strong enhancement of the electric field on the land side, which will potentially increase GIC considerably in the land segment compared to a similar situation far from the coast. Merely using the background E-field will underestimate the potential drop along the landside of the system, while it will overestimate the ocean side of the system.

**GIC calculations:**

The intensity of electrical fields from solar storms can be classified to moderate (20-100 years, 2.5 V/km), high (~100 years, 5 V/km) and extreme (>100 years, 10-20 V/km). Even minor geomagnetic events can cause operational difficulties. A minor electrical field (0.3 V/km) was estimated in November 2021 in Mid-Norway and resulted in disconnection of a transformer due to consequences of saturation. GIC in the neighboring transformer was measured to about 60 A.

If considering a simplified electrical circuit of the 67 km long Krafla subsea power cable, indicative values for GIC and reactive power consumption (three-phase, three-legged, core form transformer, 500/230 kV, 300 MVA) are calculated as follows:

- Moderate storm (2.5 V/km): 50 A, 15 MVAR
- High storm (5 V/km): 100 A, 30 MVAR
- Extreme storm (10-20 V/km): 200-400 A, 60-120 MVAR

If the (accumulated) e-field increases due to the fjord placement, calculated GIC will also increase. Currents higher than 150 A (50 A/phase) is in literature considered as "high peak GICs".

#### **Further work:**

Recommended further work for the Krafla subsea power cable is:

- Establish a complete GIC model/e-field model of the actual coastline and fjord.
- Perform system evaluations with respect to GIC vulnerability in the region where the Krafla subsea power cable is connected to shore and evaluate if mitigation actions are required. Mitigations can be on the cable side, the transformer and/or on the transmission system side. This must be performed by, or in close cooperation with, Statnett. The maximum allowable reactive power consumption and other limits of the Krafla system is relevant to procure appropriate equipment.
- Perform GIC measurements on existing subsea cables in the same geographical area as the Krafla subsea power cable.
- Develop a relationship between GIC measurements and available space weather data.

## 2 INTRODUCTION

This report focuses on geomagnetically induced currents (GIC) that can be induced in long subsea power cables. GIC is not a threat to the power cables themselves, but can become an issue if the transformers at each end of the cable have solid bonded (grounded) neutrals via transformer neutral or reactors. The main issue with GIC is related to saturation of transformers, that can increase the reactive power consumption, voltage drop in the power grid and overheating of the transformer. This can cause an escalating situation with increased overloading in the transmission grid, disconnections and stability issues and distortion. An extreme event with a duration of several days could initiate power system collapse and equipment damage, leading to severe social consequences.

The aim of the report is:

- to perform a literature survey and compile a list of technical references on geomagnetically induced currents.
- perform an initial, high-level assessment of realistic consequences of GIC.
- identify any additional GIC-related aspects relevant for NOA Krafla.

Section 3 is dedicated to solar storms and how they affect the power grid, with emphasis on consequences of GIC, mitigative measures, transformers, power system modelling and GIC measurements. An essential part of the work is to evaluate if the electrical field across the subsea power cable (and thus GIC) is influenced by the conductive seawater. This is considered in Section 4. Finally, in Section 5, the magnitude of GIC and reactive power consumption of different transformers is estimated for a simplified equivalent electrical circuit of the Krafla subsea power cable.

It must be noted that the available literature is mainly directed towards transmission system operators (TSOs). The Norwegian TSO is Statnett. As Statnett can disconnect the power supply to Krafla, for example due to disturbances from GIC events, GIC mitigations must be coordinated in close collaboration with them. Only Statnett has real time overview of available capacity in the transmission grid and the authority to provide mitigation measures so that Krafla is not disconnected unintentionally.



## 3 SOLAR STORMS AND HOW THEY AFFECT THE POWER GRID

### 3.1 Introduction

There are many good publications focusing on GIC: how GIC affects the power system, mitigations, historical GIC-events and lessons learned from these and how to perform detailed thermal modelling of transformers and the power grid during GIC events. Of special interest are reports published by CIGRE [1] and, focusing on North-America, guidelines and recommendations by the institutions EPRI [2]–[8] and NERC [9], [10]. The first reference by NERC is a high-level summary of the work that EPRI completed on the topic in 2020, with reference to several EPRI articles. An EU-project, European Risk from Geomagnetically Induced Currents (EURIGIC), ran between 2011 and 2014, [11]. It was coordinated by the Finnish Meteorological Institute.

The CIGRE technical brochure, [1], mainly concentrates on digitally measured magnetic field environments throughout the world, with emphasis on the larger geomagnetic storms. Most of the brochure is evaluation of datasets. It goes more in detail on the different types of plasma (solar wind/storm) and difference between solar flares and Geomagnetic disturbances (GMD). The magnetic fields can be characterized as Sudden Impulse (SI), Electrojet and Coronal Hole High Speed Stream (CHSS) waves.

#### 3.1.1 GIC classification

The effects on the power systems are separated into four main areas of concern, [1]:

1. An intense short event (10-60 s) that initiates spurious or correct relay tripping.
2. Sustained high peak GICs >50 A/phase for ~1 to 60 min that can cause overheating of transformers
3. Moderate GICs of 40 A (in the neutral) can cause heating of transformers, initiating degradation
4. Regular (nightly) GMDs that can cause low energy degradation, leading to failures within months.

#### 3.1.2 From space weather to GIC

Geomagnetic disturbances (GMDs) are initiated by plasma (commonly called solar wind or solar storms) from the sun reaching the Earth and interacting with the magnetosphere – the zone of the significant magnetic fields of the Earth.

Geomagnetically induced currents (GIC) are produced by a naturally induced geoelectric field during geomagnetic disturbances. Phenomena from the Sun, such as Coronal Mass Ejections and Corotating Interaction Regions are strong transients in the solar wind that give rise to intensified space weather. In the event of such transients interacting with Earth's magnetic field, so called Geomagnetic Storms occur. During geomagnetic storms the current system flowing within the magnetosphere-ionosphere system is enhanced, with strong (>10<sup>6</sup> A) currents flowing horizontally in the upper atmosphere, thus giving rise to larger than normal geomagnetic disturbances on the ground. The geomagnetic disturbances set up an electric field in the Earth's Crust. This electric field is the main driver for the induced electrical currents that will flow through earth and conductive materials, such as electricity transmission lines, oil and gas pipelines and non-fiber communication cables.

The induced voltage at the Earth's Crust is correlated to the size of the currents in the atmosphere (and thus the magnetic field), together with the electrical conductivity in the Earth's Crust. As the atmospheric currents have very low frequencies, and the Earth at many locations low conductivity, the skin depth for GIC become large (several hundred kilometres). The electrical field does not only exist in the Earth's Crusts. Onshore, it is common to assume that the electrical field at the Earth's surface is similar to the induced field in the transmission lines at that location.

The number of sunspots indicate the likelihood and frequency for intense space weather. The sunspots are magnetic active regions in the outer layers of the sun. Solar storms often origin from or close to the sunspots. Observations of sunspots vary in 11-year cycles, with a new maximum around 2023-2025. The worst events may however happen independent of the most active periods.

### 3.2 Consequences of GIC

A summary of how GIC effects of the power grid is given in Table 3-1. Note that mitigations to GIC consequences are given in Section 3.4.

Table 3-1: Summary of effects of GMDs and GICs on power systems, [12].

Transformer saturation	GIC acts as a DC current source which determines a bias in transformer operation, shifting it to the saturated region of the magnetization curve.
Reactive power losses	Saturated operation yields augmented current demand which generates linearly increasing (i.e. with the current) reactive power consumption.
Harmonics	Operation in the saturated region is highly non-linear and distorted, generating harmonics in current/voltage waveforms.
Transformer overheating	The excess flux induced by saturation flows externally to the core into the transformer tank can generate local hot spots of over 170°C.
Generator overheating	Generators are subject to harmonics and voltage unbalance caused by transformer saturation. The ensuing harmonic currents can potentially generate excessive heating and mechanical vibrations, although no serious generator damage due to GICs has been documented.
Protective relaying issues	Relays (such as differential protection relays) reacting to the peak value of the current are sensitive to the harmonics injected by saturated transformers and can erroneously trip.  The differential protection relays can also trip unintendedly due to large difference in reactive power consumption on the primary and secondary side, since the transformer consumes more reactive power during saturation. In other words, even if the protection measures correct reactive power, it may trip since the protection believes there is a short-circuit in the transformer since the reactive power into the primary side is not equal to the output at the secondary side.
Telecommunication systems	GMDs affect phone lines and Internet cables, however optical fibers (increasingly used nowadays in the high band width lines of SCADA networks) are immune to electromagnetic interference. Satellite systems (used in WAMS) are directly prone to interference from GMDs.  Very long fiber optic cables have repeaters at regular intervals that are supplied by dedicated power cables. These may be exposed to GIC.

### 3.3 Examples of historical GIC-events

The main reference in this section is [12].

#### 3.3.1 Norway

At least one transformer has been disconnected a few times due to GIC presence but power supply has not been lost. In the Norwegian 420 kV system, GIC is measured on a weekly to monthly basis in the range 5-15 A. This is based on SINTEF measurements in a transformer in Mid-Norway (2019 to present), but also from Statnett internal measurements at a few other locations the previous years. The maximum measured GIC was on July 14 1982 in Aura substation, where at least 100 A (maybe up to 300 A) was measured [13]. 4 transformers and 15 lines tripped in Sweden, [14]. The reference says that GIC of about 300 A was measured for a few minutes in Sweden in 2003.

#### 3.3.2 Canada/US

March 13, 1989, GIC created excessive harmonics in the transformers and in the bulk transmission network in Canada/US. This caused a nine-hour outage of Hydro-Quebec's electricity transmission system. The harmonic currents flowed into nearby static VAR compensators and loaded the capacitors to such an extent that the protection systems sensed an overloading and took the static VAR compensators off-line to prevent equipment damage. Seven SVC tripped and shut down. This, coupled with the increased reactive-power demand of the saturated transformers, contributed to severe voltage regulation problems. 10 out of the 24 capacitor installations were lost in US states.

One transformer (22-500 kV) had to be replaced due overheating from half-cycle saturation. A thoroughly investigation of a 350 MVA 500-138 kV transformer was performed March 16, 1989 because of high gas levels in the transformer oil, a sign of unusual core and tank heating. External inspections showed 4 patches of paint burnt by intense heat from stray magnetic flux. Subsequent studies estimated that 80 A of GIC entered the transformer. The steel core was not designed for such abnormal conditions. Heat from the flux reached 400°C in some hot spots.

#### 3.3.3 Sweden

Seventeen major flares erupted on the sun between October 19 and November 5, 2003. The unusually high geomagnetic activity caused a number of disturbances in the Swedish high-voltage power transmission system. Circuit breakers for several power lines and transformers were tripped by the low-set residual overcurrent relays. More than 50% of the relay operations came from the second harmonic residual overcurrent relays. An electronic low-set definite time overcurrent relay tripped the circuit breaker and caused power outage in Malmö.

#### 3.3.4 UK

During the last decades, the UK electricity supply system has experienced significant GIC effects, especially in 1982, 1989 and 1991. During these events only two transmission network transformers were damaged as the events did not persist for sufficiently long periods; however, the potential for wider disruption was evident.

1. Large reactive power swings of about 50–70 MVar on individual generators.
2. Voltage dips on the 400 and 275 kV grid of up to 5%.
3. Distribution system voltage dips of up to 20%, with an average value of 5%.
4. Repeated triggering of generator negative sequence current alarms.
5. Large real and reactive power swings in interconnections between England and Scotland.
6. Failure of two identical 400-132 kV, 240 MVA transformers at Norwich Main and Indian Queens.

7. Increased number of failures of the communication channels employed for protection and energy management system remote terminal unit (RTU) communications.
8. Recorded transformer neutral DC currents of 5–25 A at certain substations.
9. Very high levels of even harmonic currents due to transformer saturation.

### 3.4 Mitigate consequences of GIC

The main principle to mitigate consequences of GIC derived from [15] is given in this section. The report also includes a more detailed assessment. List of mitigation options are also available in [1], [12], and not least in [4, Ch. 8.7.3]. In general, consequences of solar storms can be reduced by making the power grid more resistant to the effects of GIC currents, or by limiting the GIC that is induced by the solar storms.

Reduce GIC:

- Install components blocking or reducing GIC (resistors, inductors, capacitors).
- Operate the power grid such that the amplitude of GIC is limited

Increased robustness:

- Operate the grid during solar storms with sufficient safety margins with regards to surplus active and reactive power. The grid can then handle the increase of reactive power consumption and possible disconnections without cascading disconnections, such as overload.
- Install transformers capable of handling larger DC currents with less saturation, so that harmonics and increased reactive power is reduced
- Ensure that the transformers can manage increased losses as a consequence of GIC without excessive thermal overloading.
- Ensure that all relays are correctly coordinated such that there is no unintended (cascading) disconnection as a result of increased harmonics and increased reactive power.
- Operate and dimension the grid so that the components (e.g. capacitor banks) are not as easily overloaded with high content of harmonics.
- Ensure that atmospheric disturbance is considered in design of control systems and critical components.
- Operate the grid with temporary reduced loading on critical components during solar storms to avoid disconnections.

### 3.5 GIC and breakers

The main text in this section is from [4].

In an inductive network, current can only be interrupted when it becomes zero during a 50/60 Hz cycle. A high voltage network is largely inductive, and circuit breakers designed to interrupt fault and load currents rely on a zero current crossing to initiate the process of successful arc quenching and current interruption.

If the magnitude of GIC is small compared to the magnitude of currents to be interrupted during a fault a zero crossing in the current to be interrupted will always take place. On the other hand, finding a zero crossing could be a problem if the magnitude of GIC exceeds the peak value of current in a lightly loaded circuit. In such a scenario, the arc between the poles of the circuit breaker would not be interrupted, and could, in principle be sustained for seconds or minutes and eventually damage the circuit breaker.

If a breaker fails to clear a fault, the protection and control system would either detect the improper position of the breaker pallet or the persistence of fault current, and a “breaker failure signal” would initiate the backup current interruption process. In the case of load current interruption, under very large GIC conditions, the contacts would be in the correct position (i.e., open), but the current through the breaker may not be enough to trigger a “breaker failure” signal.

This is a low probability event, but merits additional research and consideration, especially on the part of circuit breaker manufacturers, and protection and control experts.

The nominal current to Krafla subsea power cable is around 830 A, see Table 5-1. This means that zero-crossing will take place as long as GIC is less than about 1170 A ( $\sqrt{2} \cdot 830$ ). From Figure 5-2, expected GIC in an extreme event is estimated to be about 410 A. Thus, if Krafla is running at more than 35% load, there will (always) be zero-crossings.

The load current through the reactor is normally smaller compared to the current in the transformer. Depending on the magnitude of GIC through this component (not estimated in this report), the topic may be more relevant at this location. An evaluation of the probability of large GIC and the following consequences could be performed.

## 3.6 GIC and transformers

### 3.6.1 Standards

There are at least three important transformer standards that are relevant for exposure to GIC, [16]. IEEE/ANSI standard C57.12 [17] and IEC standard 60076 [18] provide for time limits on overexcitation of the transformer. In addition to these standards, IEEE/ANSI C57.110 [19] also defines limitations for transformers exposed to non-sinusoidal currents. In 2015, a guide for geomagnetic disturbances on transformers was published as IEEE C57.163, [20].

### 3.6.2 Full scale measurements

[21] refers to two full size experiments performed by Hydro Quebec (550 MVA) and FINGRID (400 MVA), in which very large 1 – phase and 3 – phase power transformers were injected with high levels of DC (75 Amps for 20 minutes and up to 200 Amps for 30 minute intervals, respectively). Temperature rises were measured in windings and structural parts of the transformers. It was found that the temperature rises were in a reasonable range in spite of the high levels of DC applied continuously for long durations. As concluded by these studies, even high levels of GIC currents should not cause transformer damage. An earlier experimental study of the effect of DC on power transformers was conducted by Tokyo Electric Power Corporation, in collaboration with Toshiba, Hitachi, and Mitsubishi. The study tested several small-scale models of core form as well as shell form transformers with different core types. Based on the results from these small-scale models, measurements were made on two large– scale models of 1 – phase, 3 – legged 1000 MVA / 550 kV core form and shell form transformers. These transformers were tested with DC level up to 66 Amps which corresponds to 400 – 600 Amps / phase for the corresponding full size transformers. The DC was applied for up to 20 – 30 minutes continuously. The leakage flux and temperatures were measured in windings and structural parts of these transformers. The maximum temperature rise measured after 30 minutes of applying such large magnitudes of DC continuously, was approximately 110 °C in both the Tie–plate for the core form transformer and the core support in the shell form transformer. The study concluded that because of the short duration of these temperatures, the transformer life would not be significantly affected. Also, the very short duration of GIC would not allow hot spot temperatures to rise to a fraction of these temperatures.

### 3.6.3 Design

In [22], power losses in the three-phase three-legged transformer is evaluated. GIC and converter modulation effect are two main causes for DC magnetization in power transformers. Tests and simulations are performed on such transformer.

[4], [23] are two of several publications that provide an evaluation of different power transformer designs focusing on how susceptible they are to GIC. Single phase transformers are more sensitive than three phase transformers. Both single phase transformers and three phase transformers come in many different core designs, and they have differences in GIC susceptibility. The two most important types of three phase transformers are three legged and five legged. There will flow the same amount of GIC through three legged transformers as through a five legged. The five legged saturates more easily than the three legged.

As mentioned in the previous section, [4, Ch. 8.7.3], provide a good list of mitigation measures by transformer design.

### 3.6.4 Specifications in Sweden, Finland and Norway

Svenska Kraftnät's policy is that transformers, as far as possible, must be of the three-legged three-phase configurations, [16]. They require that the new three-legged core-form transformers shall have the withstand capacity for direct current of 200 A for 10 min with simultaneous full load current. Other protection options, when the requirement is not possible, are ground fault trips set at 120 A of zero (due to DC component), differential protection and temperature and dissolved gas monitoring.

In Finland, series capacitors have been installed on all long 400 kV transmission lines, [16]. The report states that "Only three-legged and five-legged, 3-phase, core-form transformers are used in the Finnish grid, which have the highest magnetic reluctance of all transformer types and are therefore most resistant to GIC effects". It is not known what transformer types these two are compared to, such as shell-type or single core transformers. It is evident that the three-legged is more reluctant to GIC than five-legged in respect of less reactive power consumption (but not necessarily thermally), as indicated in Section 3.6.3. The transformers on the 400 kV and 220 kV grid are grounded using current limiting reactor coils, which dampens GIC magnitudes (through the effect may be limited since GIC is low frequency and the resistance will be the main restrictor). Relay settings have been set to higher levels to reduced mis-operation under GIC conditions.

In Norway, no public information is found. From hearsay, newer transformers for the 420 kV grid (solid bonded neutral) are specified to handle about 100 A for a specified time (10-15 minutes). A 420 kV transformer in Mid-Norway has been disconnected by the protection system about once annually the last few years due to GIC effects. The line length is less than 100 km in each direction to the nearby transformer stations.

### 3.7 Power system modelling of GIC

The fundamentals for power system modelling of GIC is for example described in [3], [4, Ch. 8], [12], [24]. A high-level overview of the modelling is given below:

1. Establish a simplified GIC-network, i.e. a DC-network of (at least) relevant lines and transformers.
2. Establish a philosophy of geoelectric field distribution. As a start, a simplified approach with a uniform direction and magnitude of the geoelectric field of, say 2, 4, 10 etc. V/km, can be used.
3. Calculate GIC based on 1) and 2).
4. Calculate reactive power losses due to GIC
5. Assess equipment performance to know the stresses imposed on equipment and their withstand characteristics when exposed to those stresses.
6. Perform power system modelling and analysis to ensure that the system can operate under GIC events: sufficient busbar voltage, active and reactive power flow, no overloading of transmission lines and transformers, etc.

According to [3], several open source and commercially available software packages have included many of the GIC calculations procedures described herein. Powerworld Simulator, [25], and EPRI OpenDDS, [26], are two such tools. One software method is described in [27].

### 3.8 Measure GIC and correlate GIC to space weather measurements

An essential part of a GIC flow mitigation program is to install monitors to measure GIC flow and harmonics on a continuous basis. Monitors are a key source of real-time information that can guide system operators in determining real-time response. The monitors can also provide valuable historical records of previous space weather activity that can be evaluated and used into power system planning and analysis. Coupled with alerts and warnings, the monitoring data can show that a GMD event is imminent or in progress and can spur action. [4], [28] emphasizes in more detail the importance of monitoring GICs.

#### 3.8.1 Vendors

There are a few vendors of GIC sensors, such as Weidmann (InsuLogix GIC), Dynamic Ratings and Advanced Power Technologies, see Figure 3-1. All vendors deliver sensors with different range, typically around +/-50 A and +/-500 A. GIC is measured on the transformer neutral with a hall effect sensor (transducer) and low-pass filter.

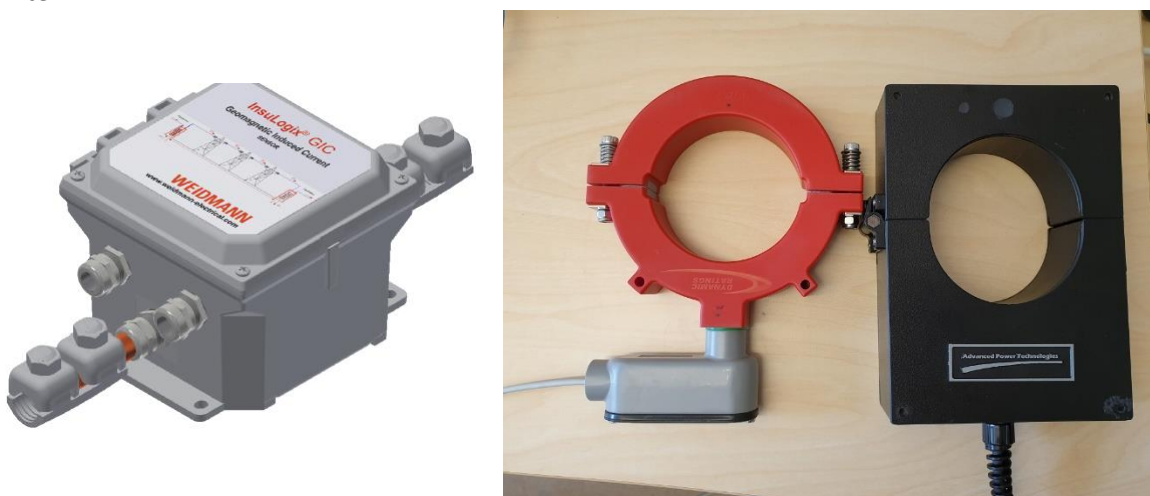


Figure 3-1: GIC sensors from Weidmann (left), Dynamic Ratings (centre) and Advanced Power Technologies (right).

### 3.8.2 Measurement set-up

Different literature focus on measurement set-ups and some compare measurement to geomagnetic activity, such as [1, Pt. Appendix B], [13], [29]–[35]. [35] give an overview of GIC measurement data from 2001 of up to 58 transformers in New Zealand. [32] and [30] presents five years of GIC measurements in the Austrian grid, focusing on two events in 2017 and 2021 where GIC of 30 and 50 A was measured. It is worth noticing that Norway is closer to the northern lights (more exposed to GIC) zone than New Zealand and Austria.

Ideally, the transformers that have the transducers installed should also have temperature recorders and online gas monitors associated with them. This will enable GIC events to be correlated with any observable physical changes within the transformer and provide an indication of whether any deterioration of transformer condition can be attributed to GIC's. Other quantities that can be optionally measured, and be of benefit are, [1]:

- 2nd to the 5th harmonic on transformer input currents and voltages. The even harmonics can be used as an early warning of transformer partial saturation
- Reactive power of the transformer primary and secondary. The transformer magnetizing (MVAR) load can be calculated, which provides an indication of saturation level and allows the operator to unload the transformer if they exhibit even harmonics and /or large excitation loading.
- Transformer tank temperature, as an indication of large leakage flux
- Transformer tank's acoustic sound, as an indication of large core currents.
- Transformer tap positions

### 3.8.3 Measurements in Norway

[29] presents two years of GIC measurements on a 420 kV transformer, together with measurements of variation of the geomagnetic field (dB/dt). A network of magnetometers, for local measurements of the Earth's magnetic field, are placed throughout Norway. Data from these instruments are available from Tromsø Geophysical Observatory, a part of UiT – The Arctic University of Norway. GIC up to 60-70 A was measured. The distance between the transformer station and neighboring stations is about 50 km (southern direction) and 70 km (northern direction). The report concludes that there is a correlation between GIC and dB/dt. Each of the variables fluctuate at the same time instances. However, the magnitude and shape has not the same clear correlation. The authors did find a very good correlation between GIC and the geomagnetic E-field, that is not presented in the report. Therefore, by measuring GIC for a limited time to calibrate e-field models, GIC can be estimated locally by using data from existing magnetometers. An important conclusion from the report is that transmission lines with east-west orientation are as vulnerable to GIC as transmission lines oriented north-south (based on the measurements of this specific transformer).

## 3.9 Magnitude of B- and E-fields

In this section, examples of expected order of magnitudes of B- and E-fields are given.

Calculations performed by the Finnish Meteorological Institute, [36], conclude that mainland Norway between 1994 and 2011 likely was exposed to an electrical field of maximum 5 V/km during a solar storm. The report estimates that the worst scenario during hundred years will be less than 10 V/km. In [37], [38], 10 V/km is considered moderate and 20 V/km extreme. On the other hand, a theoretical maximum at these stations in a 100-year period was found to be in the range 5.9 – 7.6 V/km in [39].



In the 1989-event in the US, peak 1-min-resolution geoelectric field amplitude was estimated to, [40]:

- 22 V/km in Maine
- 19 V/km in Virginia
- <0.02 V/km in Idaho.

The maximum and minimum ratio between E-field (V/km) and dB/dt (nT/min) is in [1] calculated to:

- 0.003 (V/km)/(nT/min)
- 0.008 (V/km)/(nT/min)

In Mid-Norway, dB/dt of up to ~700 nT/min was recorded in October 2020 and November 2021, [29], indicating E-field in the range 2-6 V/km. This is however a decade higher than the 0.3 V/km estimated in Section 4.3.

## 4 SEAWATER AND E-FIELD

The literature associated with GIC in landbased pipelines and power grids is substantial. On the other hand, little work has been done related to subsea cables and the GIC impact on these. As on land, the induced E-field is key to assessing the GIC that will flow in such systems, but the high conductivity of the sea water, varying sea depth and transition from land to sea, introduces additional challenges to the problem.

### 4.1 Depth effect

In particular the effect of a coastline is important for GIC estimates. The coastline represents an abrupt change in conductivity from relatively low conductivity on land to a relatively high conductivity in the ocean. Induced currents flowing in the ocean towards or away will therefore be higher than on land, and will thus build up a potential peak along the coastline to maintain a divergence free current. Thus, the geoelectric field on the land side will increase [41], and the effect will be seen far inland, see Figure 4-1.

Several early studies exist related to long wires across long ocean stretches. E.g. [42] analysed GIC in a transatlantic communications cable under quiet conditions, and [43] studied the potential variations across a similar cable during geomagnetic storm conditions.

Quantitative modelling of the E-field on the ocean floor has only been studied by a few authors. [44] and [45] established and modelled the electric field below the ocean based on realistic variations in the magnetic field at high latitudes. However, in these papers no coastline effect was considered.

[44] demonstrated how the sea depth has a strong effect on the magnitude of the electric field, where there is a strong attenuation of the field for large depths. These findings were further quantified and investigated by [46].

[47] introduced a coastline situation for the first time in subsea GIC modelling. His method was furthermore refined by [48] and [49]. A study by [50] modelled the voltage over a transoceanic communications cable during geomagnetic storms.

For power transmission between an installation offshore and land, several aspects need to be summarized. In our particular case the offshore location is about 260 km from the coast and in a fairly shallow part of the Ocean, the North Sea with an average depth around 100 m. There is also a seabed transmission line going inland for 60 km along a fjord. Although, demonstrating the importance of the coastline effect, the papers mentioned above have a rather fast increase toward large depths from the coast, which renders the modelling unrealistic compared to the North Sea situation. Recently [51] established a modelling framework to investigate the effect of a coastal situation with a shallow offshore continental shelf, a so-called thin shell model. This was then applied by [52] to investigate a coastal scenario including a shallow (200 m) transition region between land and deep ocean, which is similar to the North Sea. Here they demonstrate how the geoelectric field will increase towards the coastline on the land side, and how the effect of the E-field increase will be seen further inland as the distance to the deep ocean increases. In a simple GIC calculation they demonstrate that in the case where the distance to the continental shelf is 500 km (which is very similar to the North Sea Coast), the GIC will be more than 200 % higher than under same conditions without an ocean. [53] successfully used the same technique including the coastal effect to simulate GIC in the Guangdong Province of China. The coastal effect is demonstrated in Figure 4-1.

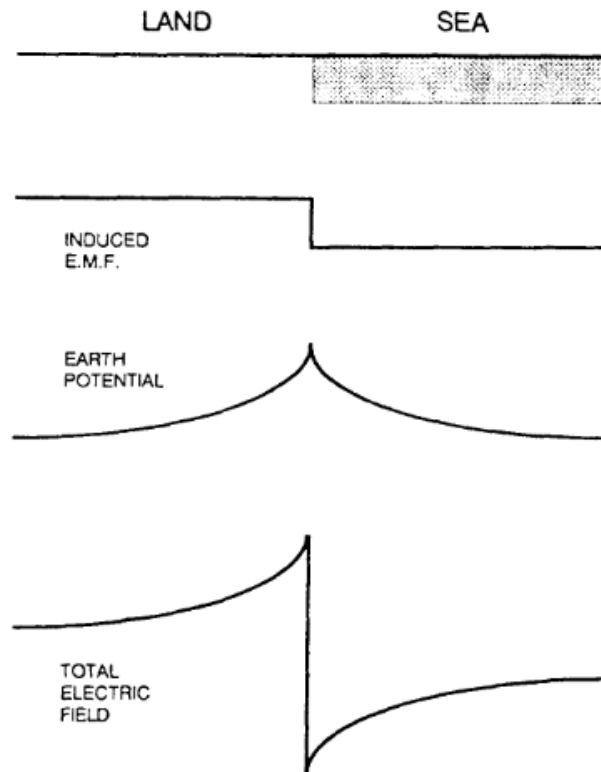
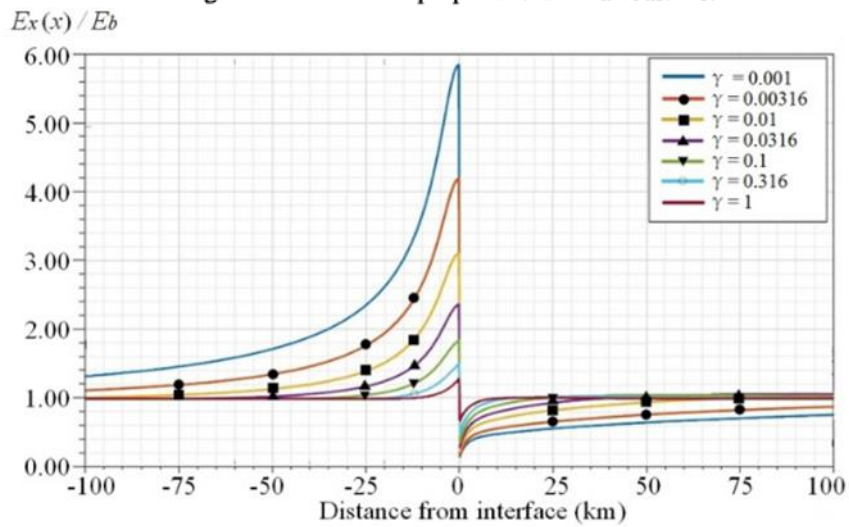


Fig. 2. Electric fields perpendicular to a coastline.



**FIGURE 10.** Normalized geoelectric field at the surface of the Earth in the thin shell model with  $f = 0.001$  Hz and  $\gamma = 0.001-1$  S/m.

Figure 4-1: Conceptual drawing of the coastal effect (upper, from [41]) and model result of the same at a coast with a long and shallow continental shelf (lower, from [51]).

## 4.2 E-field of Krafla

A complete model treatment of the Krafla development with respect to GIC is beyond the scope of this work. However, a simple first order assessment is possible. For the GIC estimates one needs to know the magnitude of the geoelectric field in the area of interest. This field can be estimated from ground based magnetometer data and a model of the earth conductivity. The most basic approach, which does not take the coastline into account and therefore is a clear underestimation of the real situation, is a plane wave approximation with a half space, layered Earth for conductivity, see e.g. [54]. Below (Figure 4-2 to Figure 4-5) we show E-field estimates from four magnetometer stations in Southern Norway, Karmøy (KAR), Harestua (HAR), Solund (SOL) and Dombås (DOB). We have used the same conductivity model as [39].

Fitjar, where the cable goes out into the North Sea, is approximately halfway between SOL and KAR. The two “inland” stations, DOB and HAR, have been included for reference to show the situation without possible electric currents in the ocean parallel to the coastline distorting the signal measured by the magnetometers and, thus, introducing uncertainties in the E-field estimates (this effect should not be confused by the coastal effect discussed above). Although, different, the E-field estimates on the four locations are fairly comparable with respect to magnitude. This particular data set was chosen since Statnett experienced a transformer tripping in mid-Norway with GIC measured in the order of 50 A that particular day. Estimates of the geoelectric field in mid-Norway amounted to  $\sim 0.3$  V/km during this event. As can be seen in the Figures 2-5, stations further south saw comparable fields in the range 0.1 – 0.7 V/km.

[39] made a comprehensive assessment of geoelectric fields across Norway as well as an evaluation of GIC in the national power grid. They found that the highest geoelectric fields experienced at KAR and SOL in the period 1994-2011, were 3.3 and 4.1 V/km, respectively. A theoretical maximum at these stations in a 100-year period was found to be in the range 5.9 – 7.6 V/km. In other words, the case that caused a transformer tripping in mid-Norway is far from the worst-case scenario in terms of geoelectric fields. It should also be noted that [39] did not take any coastal effects into account, either.

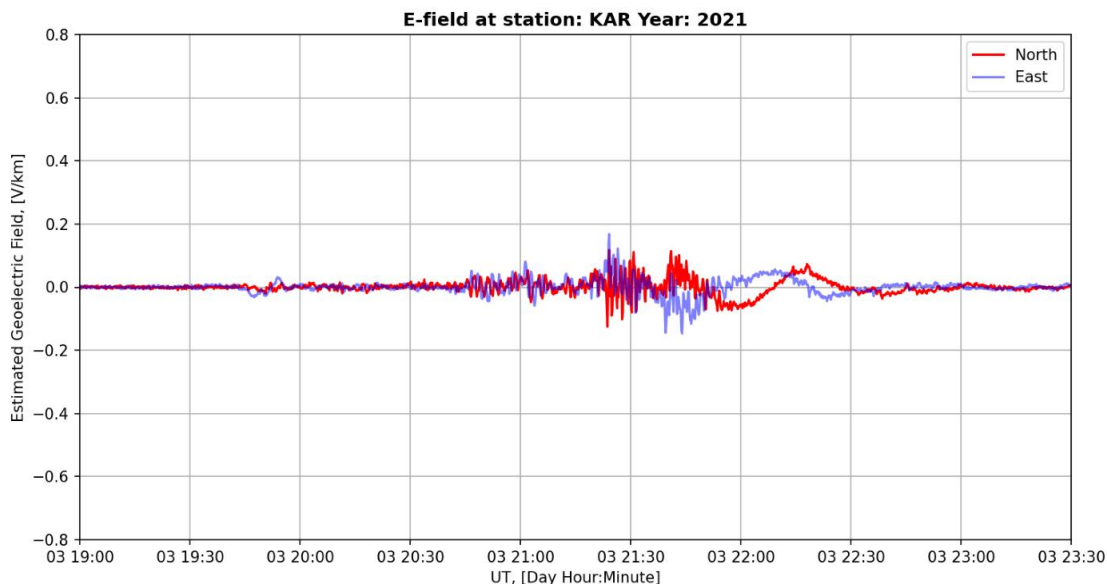


Figure 4-2: E-field estimate at Karmøy magnetometer on November 3. 2021.

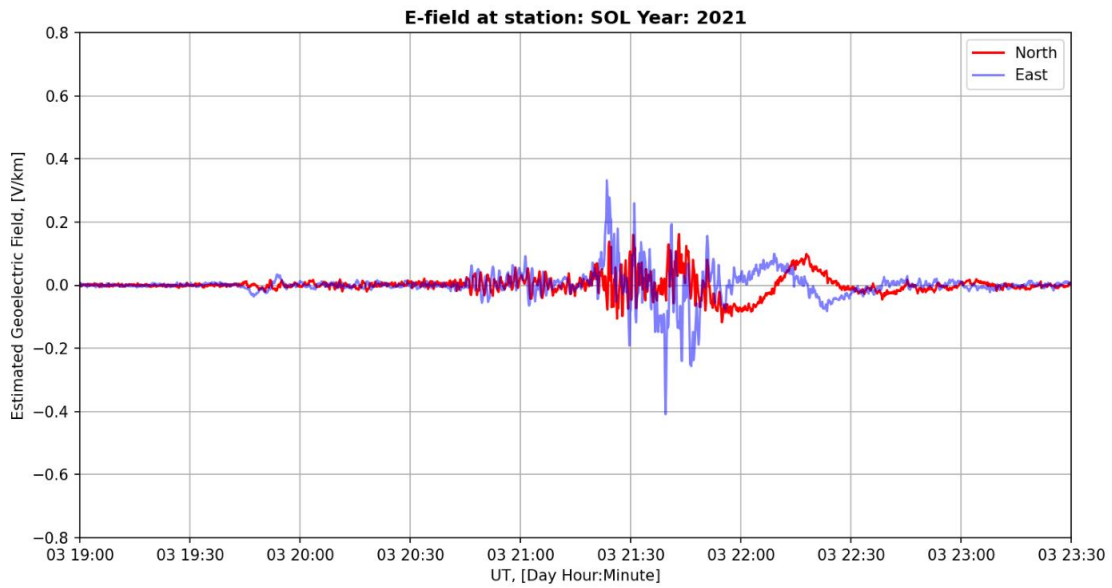


Figure 4-3: E-field estimate at Solund magnetometer on November 3. 2021.

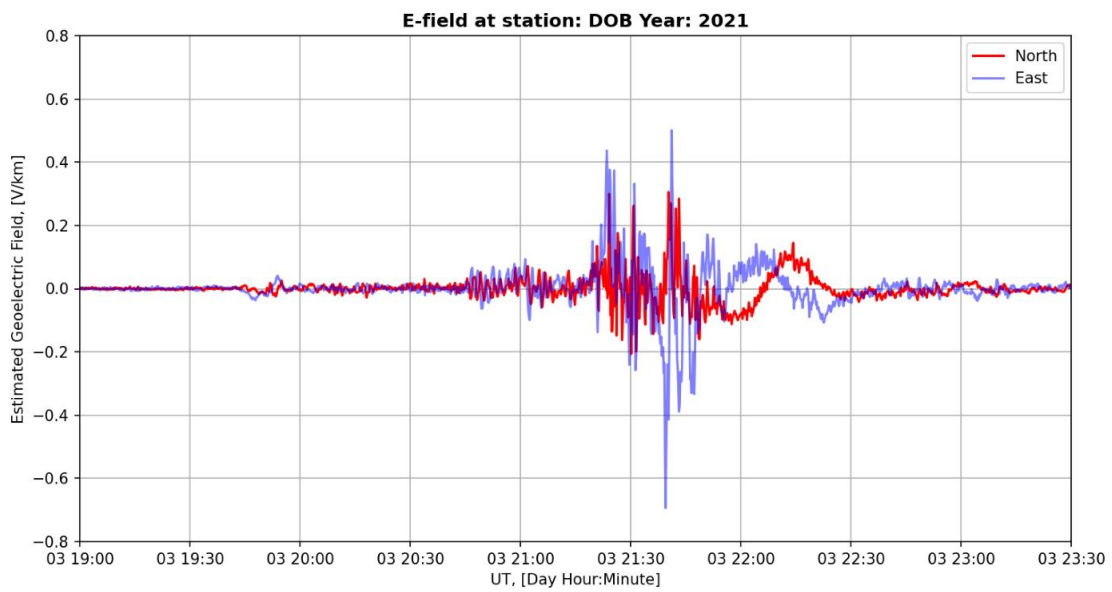


Figure 4-4 E-field estimate at Dombås magnetic observatory on November 3. 2021.

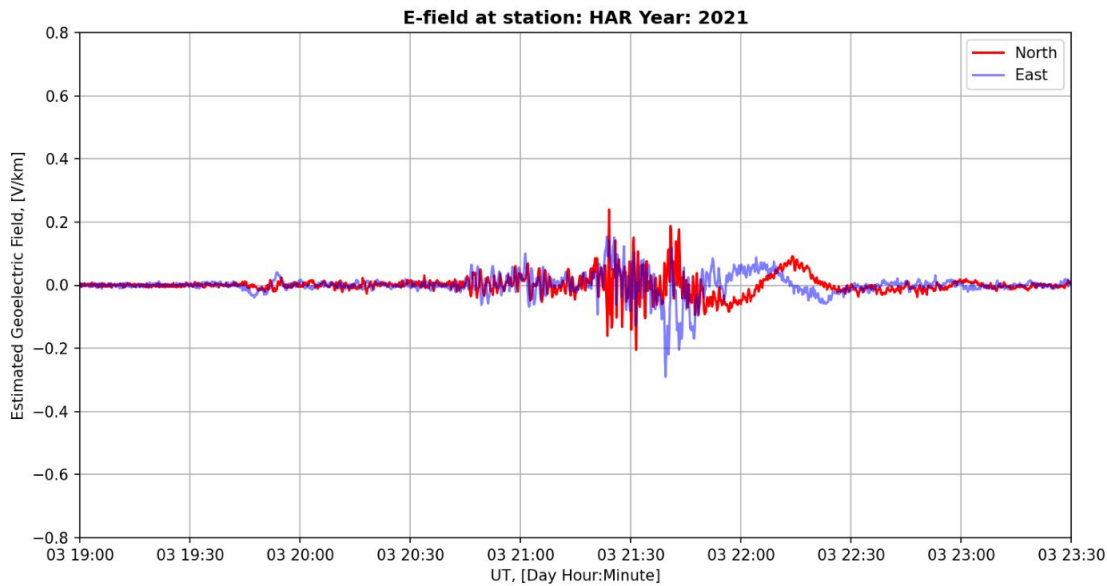


Figure 4-5: E-field estimate at Harestua magnetometer on November 3. 2021

### 4.3 Coastal effect

The sea depth along the cable will vary between 0 and 600 m in the fjords and around 100 m off the coast. Based on the findings of [46] (i.e. their Figure 4-1) we argue that the ocean can be neglected, as an attenuator of the electric field, in the North Sea owing to the shallow depth: Their study finds that only sea depths beyond 1000 m contributes to any significant attenuation of the E-field. The E-field will remain within 95 % of the surface field at 1000 m. To estimate the E-field on the sea floor in our area of interest we can, thus, take the same approach as on land and use the magnetic field estimates from nearby ground based magnetometer stations. Furthermore, since 60 km of the cable runs along a fjord, where the bulk of the surroundings includes land, it is reasonable to argue that the sea can be ignored along this stretch. The scenario is therefore as follows.

In the Krafla situation, the first 60 km of the cable is on the land side of the coast. Here both ends are grounded, where the westernmost point is at the coastline. As is shown by [52], there will be a strong, exponential like increase in the E-field over this distance, which, potentially, will increase the GIC by up to 200% compared to an inland situation.

On the ocean side, the E-field will be opposed by the coastal effect and be close to zero at the coast, but increase towards the background estimate away from the coast. Thus, the integrated E-field along that stretch of cable will be less than in a similar situation in-land. At Krafla the E-field will not be affected by the coastal effect.

## 4.4 Summary

The North Sea and fjords themselves, with fairly modest depths of  $< 600$  m and an average of  $\sim 100$  m, will not contribute to any significant attenuation of the surface geoelectric field. Estimates of a background geoelectric field can, thus, be obtained from nearby magnetometers and a two layer conductivity model, as shown above.

However, the presence of the coast with a fairly shallow continental shelf which reaches far out  $> 500$  km, will introduce a strong enhancement of the electric field on the land side (Figure 4-1), which will potentially increase GIC considerably in the land segment compared to a similar situation far from the coast.

Merely using the background E-field will underestimate the potential drop along the landside of the system, while it will overestimate the ocean side of the system.

## 5 GIC ESTIMATES FOR KRAFLA

### 5.1 Introduction

The induced electric fields by GMDs will cause currents to flow in any power line segment that has a low-resistance path to ground via transformer neutrals. The integral of the electric field along a line between the two ground points is the voltage that drives the current, and the current level is given by the circuit resistance. The e-field is assumed to be uniform along the length of the cable in the GIC calculations presented in this section. The system resistance is composed of the lines (cables), grounding (ground structure and spreading resistance into the ground), and series transformer windings. The line resistance itself becomes dominant as the line length increases.

### 5.2 Electrical circuit

The total circuit resistance is estimated to 3.2  $\Omega$  for a simplified circuit, see Figure 5-1 and Table 5-1. The reactor at Årskog is not included, even though it may provide a low resistance path for GIC. The subsea cable contributes to 1/4<sup>th</sup> of the total resistance. Note that all resistances except for the groundings are divided by 3 since they actually denote phase values placed in parallel. In [5], 0.1-0.7  $\Omega$  is used as guideline for grounding resistance of substations (230-735 kV). In [36], 0.5  $\Omega$  is used on all earthing resistances (300-420 kV). For simplicity, an earthing resistance of 0.5  $\Omega$  is also assumed in this report. In [5], DC resistance of transformer windings is in the range 0.7  $\Omega$  (230 kV) to 0.2  $\Omega$  (735 kV). A value of 0.7  $\Omega$  is assumed in this report, based on 0.25% losses in each triplet of the six transformer windings.

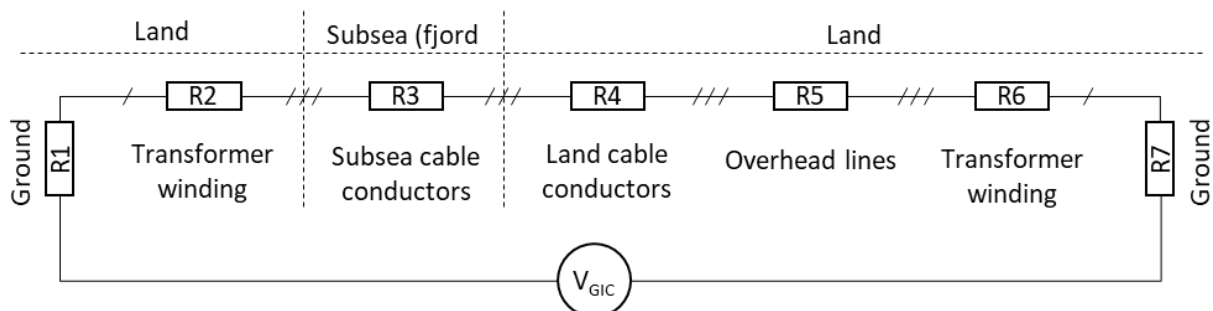


Figure 5-1: Simplified electrical circuit diagram.

Table 5-1: Resistances of circuit from Figure 5-1.

Resistor	Resistance [ $\Omega$ ]	Comment
R1	0,5	Based on literature
R2	0,7	S=180 MVA, $R_{winding LV} = 0.25\%$ (0.5 MW), V=125 kV, I=831 A
R3	0,8	500 mm <sup>2</sup> Cu, 67 km, 0.0366 $\Omega$ /km (pr. phase)
R4	0,0	1600 mm <sup>2</sup> Al, 3 km, 0.0186 $\Omega$ /km (pr. phase)
R5	0,1	800 mm <sup>2</sup> Al, 9 km, 0.0367 $\Omega$ /km (pr. phase) - FeAL 506 FALCON
R6	0,7	As R2
R7	0,5	As R1
Rtot	3,2	



### 5.3 GIC calculation

GIC can be estimated from Eq. 5-1, where  $E$  is the geomagnetic E-field (assumed uniform) over a length  $L$ .  $\cos \phi$  is the cable alignment, which is the angle between the cable direction and the vector direction of the horizontal E-field. Maximum coupling, with the line aligned with the E-field direction has a value 1, and is assumed in this report.

$$I_{GIC} = \frac{E \cdot \cos(\phi) \cdot L}{R_{tot}} \quad \text{Eq. 5-1}$$

GIC as function of the E-field, assuming 67 km length, is seen in Figure 5-2. A moderate storm (E-field of about 2.5 V/km, 20-100 years), GIC is estimated to 50 A. A large (5 V/km, ~100 years) and extreme storm, (10-20 V/km, >100 years), generate GIC in the order 100-400 A. These are moderate to high numbers. [20] defines  $GIC \geq 225$  A (75 A per phase) as the highest exposure interval. [55] says that transformers exposed to less than 225 A (75 A per phase) are exempt from the thermal impact assessment required, however, transformer thermal overheating is not the only item that needs to be considered in this context.

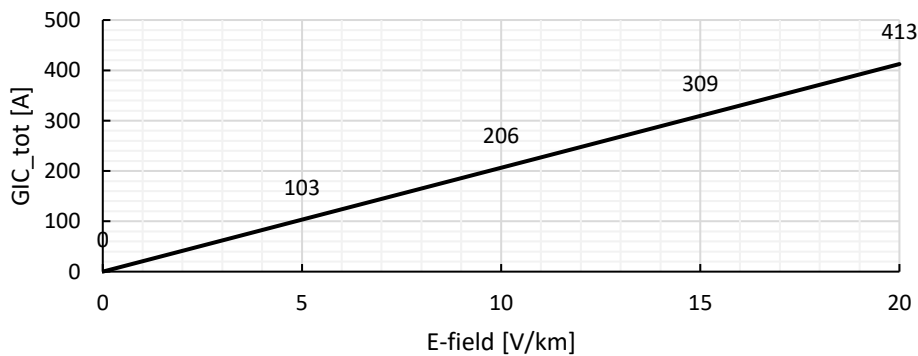


Figure 5-2: GIC (all three phases combined) as function of E-field. Length is assumed to be 260 km.

As was found by [52] in a very similar case to Krafla, the GIC can be up to 200 % larger than what is estimated based on background Electric fields owing to the coastal effect. Thus, the GIC estimates here can possibly be multiplied by 2.

### 5.4 Reactive power consumption

Once the GIC is known, the effect of the geomagnetic disturbance on the power system can be determined. As presented earlier, GICs influence power grids primarily because of the induced saturation of transformers. This in turn entails a variety of side-effects, one of the most prominent being an augmented reactive power demand at the nodes where the transformers are located. As a first approximation, the increased loading is assumed to vary linearly with the GIC flowing in the transformer, so that provided the scaling constants specific to each unit type are known, the corresponding reactive power demand can be calculated. In particular, the increase in reactive power demand can be expressed as, [12], [56]:

$$Q_{GIC} = k \cdot V_{norm} \cdot I_{GIC} = K \cdot I_{GIC} \quad \text{Eq. 5-2}$$

Where  $V_{norm}$  is the nominal voltage,  $I_{gic}$  is GIC in the transformer neutral,  $k$  is a transformer specific constant and  $K$  another transformer specific constant dependent on both transformer type and nominal voltage level. In [56], the  $K$  values are presented for analyses of a 500/230 kV, 300 MVA transformer:

- Single phase: 1.18 MVar/A
- Three-phase, shell form: 0.33 MVar/A
- Three-phase, three-legged, core form: 0.29 MVar/A
- Three-phase, five-legged, core form: 0.66 MVar/A

Based on these constants, the reactive power consumption as function of GIC (all phases combined) and E-field (assuming 67 km length) is provided in Figure 5-3 and Figure 5-4. Single-phase transformer is not included.

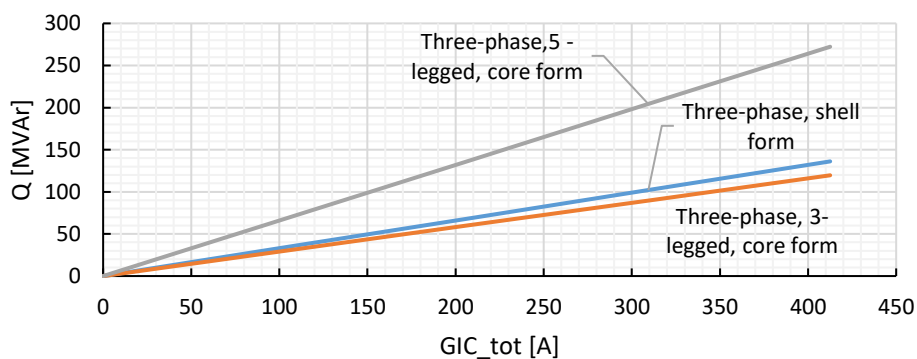


Figure 5-3: Reactive power as function of GIC (all three phases combined). Length is assumed to be 67 km.

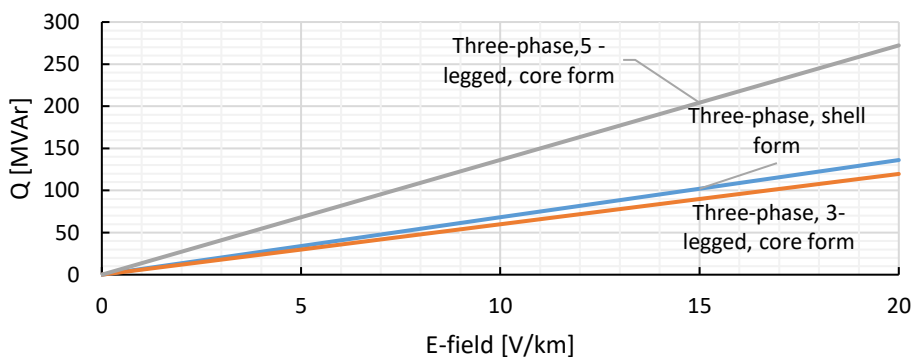


Figure 5-4: Reactive power as function of E-field (all three phases combined). Length is assumed to be 67 km.

Other side-effects of GICs such as harmonics generation, transformer overheating, generator overheating, protective relay tripping etc. are considerably more complex to model and assess, and typically require much more detailed system data as well as advanced simulation tools, and a numerical analysis can be in principle only conducted for single transformer units, [12].

## REFERENCES

- [1] Cigre, 'Understanding of geomagnetic storm environment for high voltage power grids', TB780 , C4 Power system technical performance, Nov. 2019.
- [2] NERC, 'Geomagnetic Disturbance Planning Guide', NERC, Atlanta, Georgia, Dec. 2013.
- [3] NERC, 'Computing Geomagnetically-Induced Current in the Bulk-Power System', Atlanta, Georgia, Dec. 2013.
- [4] NERC, 'Effects of Geomagnetic Disturbances on the Bulk Power System', 2012 Special Reliability Assessment Interim Report, Mar. 2012.
- [5] NERC, 'Network Applicability Project 2013-03 (Geomagnetic Disturbance Mitigation) EOP-010-1 (Geomagnetic Disturbance Operations)', 2013.
- [6] NERC, 'Geomagnetic Disturbance Operating Procedure Template Transmission Operator'.
- [7] NERC, 'Geomagnetic Disturbance Operating Procedure Template Generator Operator'.
- [8] NERC, 'Transmission System Planned Performance for Geomagnetic Disturbance Events', TPL-007-4, Mar. 2020.
- [9] EPRI, 'Research Findings for Geomagnetic Disturbance Research Work Plan', Aug. 2020.
- [10] EPRI and NERC, 'Geo-magnetic Disturbances (GMD): Monitoring, Mitigation, and Next Steps A Literature Review and Summary of the 2011 NERC GMD Workshop', California, USA, Technical report 1024629, Nov. 2011.
- [11] 'European Risk from Geomagnetically Induced Currents | EURISGIC Project | Fact Sheet | FP7 | CORDIS | European Commission'. <https://cordis.europa.eu/project/id/260330> (accessed Jun. 16, 2022).
- [12] ETH, Swiss Federal Institute of Technology Zurich, 'GEOMAGNETICALLY INDUCED CURRENTS IN THE SWISS TRANSMISSION NETWORK'. 2013. [Online]. Available: [https://www.swissgrid.ch/dam/swissgrid/current/News/2013/Schlussbericht\\_GIC.pdf](https://www.swissgrid.ch/dam/swissgrid/current/News/2013/Schlussbericht_GIC.pdf)
- [13] H. Seljeseth and O. Rokseth, 'Teknisk rapport 2958. Registrering av induserte strømmen i kraftnettet P.G.A. partikkelstrøm fra sola.', SINTEF, Elekrisitetsforsyningens Forskningsinstitutt, 1983.
- [14] M. Wik, R. Pirjola, H. Lundstedt, A. Viljanen, P. Wintoft, and A. Pulkkinen, 'Space weather events in July 1982 and October 2003 and the effects of geomagnetically induced currents on Swedish technical systems', *Ann. Geophys.*, vol. 27, no. 4, pp. 1775–1787, 2009, doi: 10.5194/angeo-27-1775-2009.
- [15] O. Mo and K. S. Thinn, 'Tiltak for å håndtere risiko og motvirke konsekvenser knyttet til geomagnetisk induert strøm i kraftnettet Rev. 2.0.', SINTEF, 2021–00209, 2021. [Online]. Available: [https://publikasjoner.nve.no/eksternrapport/2021/eksternrapport2021\\_15.pdf](https://publikasjoner.nve.no/eksternrapport/2021/eksternrapport2021_15.pdf)
- [16] E-PRO and C. Beck, 'The International E-PRO REPORT', Washington D.C., US, Sep. 2013.
- [17] IEEE, 'IEEE Standard for General Requirements for Liquid-Immersed Distribution, Power, and Regulating Transformers', IEEE Std C57.12.00™-2021, Nov. 2021. Accessed: Jun. 14, 2022. [Online]. Available: <https://standards.ieee.org/ieee/C57.12.00/6962/>
- [18] IEC, 'Power Transformers', IEC 60076.
- [19] IEEE, 'IEEE C57.110-2018 Recommended Practice for Establishing Liquid-Immersed and Dry-Type Power and Distribution Transformer Capability When Supplying Nonsinusoidal Load Currents',
- [20] 'IEEE Guide for Establishing Power Transformer Capability while under Geomagnetic Disturbances', *IEEE Std C57163-2015*, pp. 1–50, Oct. 2015, doi: 10.1109/IEEESTD.2015.7286929.
- [21] S. Girgis, K. Verdante, and K. Gramm, 'Effects of Geomagnetically Induced Currents on Power Transformers and Power Systems', 2012.
- [22] W. Wang, A. Nysveen, and N. Magnusson, 'Power losses in the three-phase three-limb transformer due to common and differential mode of dc-bias', *IET Electr. Power Appl.*, vol. 15, no. 11, pp. 1488–1498, 2021, doi: 10.1049/elp2.12113.



- [23] R. Thorberg, 'Risk analysis of geomagnetically induced currents in power systems', *Rep. Lund Univ.*, 2012.
- [24] D. H. Boteler and R. J. Pirjola, 'Modelling geomagnetically induced currents produced by realistic and uniform electric fields', *IEEE Trans. Power Deliv.*, vol. 13, no. 4, pp. 1303–1308, Oct. 1998, doi: 10.1109/61.714500.
- [25] 'Simulator GIC » PowerWorld'. <https://www.powerworld.com/products/simulator/add-ons-2/simulator-gic> (accessed Aug. 03, 2022).
- [26] NERC, 'NERC OpenDSS software'. <https://www.epri.com/pages/sa/opensdss> (accessed Aug. 03, 2022).
- [27] J. Berge and R. K. Varma, 'A software simulator for Geomagnetically Induced Currents in electrical power systems', in *2009 Canadian Conference on Electrical and Computer Engineering*, St. John's, NL, Canada, May 2009, pp. 695–700. doi: 10.1109/CCECE.2009.5090219.
- [28] EPRI, 'Monitoring and Mitigation of Geomagnetically Induced Currents', 1015938, Dec. 2008. [Online]. Available: <https://www.epri.com/research/products/1015938>
- [29] K. S. Thinn, M. G. Johnsen, and O. Mo, 'Geomagnetically induced currents in a Norwegian transformer station - Rev 2.0', 2021–01449, May 2022.
- [30] D. Albert, P. Schachinger, R. L. Bailey, H. Renner, and G. Achleitner, 'Analysis of Long-Term GIC Measurements in Transformers in Austria', *Space Weather*, vol. 20, Jan. 2022, doi: 10.1029/2021SW002912.
- [31] L. Bolduc, 'GIC observations and studies in the Hydro-Québec power system', *J. Atmospheric Sol.-Terr. Phys.*, vol. 64, no. 16, pp. 1793–1802, 2002, doi: 10.1016/S1364-6826(02)00128-1.
- [32] T. Halbedl, 'Low Frequency Neutral Point Currents on Transformer in the Austrian Power Transmission Network', Graz University of Technology, Graz, Austria, Doctoral Thesis, Jan. 2019. [Online]. Available: [https://www.tugraz.at/fileadmin/user\\_upload/tugrazExternal/83b7d5e5-91ff-43e4-aa7a-6aa30ac5c9f1/Dissertationen/\\_PhD\\_Thesis\\_Halbedl\\_Final\\_Print.pdf](https://www.tugraz.at/fileadmin/user_upload/tugrazExternal/83b7d5e5-91ff-43e4-aa7a-6aa30ac5c9f1/Dissertationen/_PhD_Thesis_Halbedl_Final_Print.pdf)
- [33] T. Halbedl, H. Renner, M. Sakulin, and G. Achleitner, *Measurement and analysis of neutral point currents in a 400-kV-network*. 2014.
- [34] J. D. Aspnes, R. P. Merritt, and B. D. Spell, 'Instrumentation System to Measure Geomagnetically Induced Current Effects', *IEEE Trans. Power Deliv.*, vol. 2, no. 4, pp. 1031–1036, 1987, doi: 10.1109/TPWRD.1987.4308217.
- [35] D. H. Mac Manus *et al.*, 'Long-term geomagnetically induced current observations in New Zealand: Earth return corrections and geomagnetic field driver', *Space Weather*, vol. 15, no. 8, pp. 1020–1038, 2017, doi: 10.1002/2017SW001635.
- [36] A. Viljanen, M. Mylly, and Finnish Meteorological Institute, 'Geomagnetically induced currents in the Norwegian high-voltage power grid: Statistics and extreme case estimations'. 2013.
- [37] Metatech, 'Evaluation of the Vulnerability of the Statnett and Svenska Kraftnat Transmission Networks to the Effects of Geomagnetic Storms', 2000.
- [38] A. Pulkkinen, E. Bernabeu, J. Eichner, C. Beggan, and A. Thomson, 'Generation of 100-year geomagnetically induced current scenarios', *Space Weather*, vol. 10, p. 4003, Apr. 2012, doi: 10.1029/2011SW000750.
- [39] M. Mylly, A. Viljanen, Ø. A. Rui, and T. M. Ohnstad, 'Geomagnetically induced currents in Norway: the northernmost high-voltage power grid in the world', *J. Space Weather Space Clim.*, vol. 4, p. A10, 2014, doi: 10.1051/swsc/2014007.
- [40] J. J. Love, G. M. Lucas, E. J. Rigler, B. S. Murphy, A. Kelbert, and P. A. Bedrosian, 'Mapping a Magnetic Superstorm: March 1989 Geoelectric Hazards and Impacts on United States Power Systems', *Space Weather*, vol. 20, no. 5, p. e2021SW003030, 2022, doi: 10.1029/2021SW003030.
- [41] D. Boteler, 'Geomagnetically induced currents: Present knowledge and future research', *IEEE Trans. Power Deliv.*, vol. 9, no. 1, pp. 50–58, 1994.



- [42] L. V. Medford, A. Meloni, L. J. Lanzerotti, and G. P. Gregori, 'Geomagnetic induction on a transatlantic communications cable', *Nature*, vol. 290, no. 5805, Art. no. 5805, Apr. 1981, doi: 10.1038/290392a0.
- [43] L. V. Medford, L. J. Lanzerotti, J. S. Kraus, and C. G. MacLennan, 'Transatlantic Earth Potential Variations During the March 1989 Magnetic Storms', *Geophys. Res. Lett.*, vol. 16, no. 10, pp. 1145–1148, 1989, doi: 10.1029/GL016i010p01145.
- [44] R. J. Pirjola, A. T. Viljanen, and D. H. Boteler, 'Electric field at the seafloor due to a two-dimensional ionospheric current', *Geophys. J. Int.*, vol. 140, no. 2, pp. 286–294, Feb. 2000, doi: 10.1046/j.1365-246x.2000.00029.x.
- [45] R. J. Pirjola, 'Modelling the electric field at the seafloor due to a non-uniform ionospheric current', *J. Appl. Geophys.*, vol. 49, no. 1, pp. 3–16, Jan. 2002, doi: 10.1016/S0926-9851(01)00095-7.
- [46] D. H. Boteler and R. J. Pirjola, 'Magnetic and Electric Fields Produced in the Sea During Geomagnetic Disturbances', *Pure Appl. Geophys.*, vol. 160, no. 9, pp. 1695–1716, Sep. 2003, doi: 10.1007/s00024-003-2372-6.
- [47] J. Gilbert, 'Modeling the effect of the ocean-land interface on induced electric fields during geomagnetic storms', 2005, vol. 10, pp. 49–53. doi: 10.1029/2004SW000120.
- [48] R. Pirjola, 'Practical model applicable to investigating the coast effect on the geoelectric field in connection with studies of geomagnetically induced currents', *HIKARI*, vol. 1, no. 1, pp. 9–28, 2013, doi: <http://dx.doi.org/10.12988/aap.2013.13002>.
- [49] T. Goto, 'Numerical studies of geomagnetically induced electric field on seafloor and near coastal zones incorporated with heterogeneous conductivity distributions', *Earth Planets Space*, vol. 67, no. 1, p. 193, Dec. 2015, doi: 10.1186/s40623-015-0356-2.
- [50] A. Mecozzi, 'Effects of geomagnetic field perturbations on the power supply of transoceanic fiber optic cables'. arXiv, Mar. 09, 2022. Accessed: Sep. 14, 2022. [Online]. Available: <http://arxiv.org/abs/2204.00560>
- [51] C. Liu, X. Wang, S. Zhang, and C. Xie, 'Effects of Lateral Conductivity Variations on Geomagnetically Induced Currents: H-Polarization', *IEEE Access*, vol. 7, pp. 6310–6318, 2019, doi: 10.1109/ACCESS.2018.2889462.
- [52] X. Wang, C.-M. Liu, D. Boteler, and R. Pirjola, 'The influence of the coast effect on geomagnetically induced currents: A modeling study', in *2021 IEEE Power & Energy Society General Meeting (PESGM)*, Washington, DC, USA, Jul. 2021, pp. 1–5. doi: 10.1109/PESGM46819.2021.9637975.
- [53] Liu, Chunming, Wang, Xuan, Wang, Hongmei, and Zhao, Huilun, 'Quantitative influence of coast effect on geomagnetically induced currents in power grids: a case study', *J Space Weather Space Clim*, vol. 8, p. A60, 2018, doi: 10.1051/swsc/2018046.
- [54] R. Pirjola, 'Derivation of characteristics of the relation between geomagnetic and geoelectric variation fields from the surface impedance for a two-layer earth', *Earth Planets Space*, vol. 62, no. 3, Art. no. 3, Mar. 2010, doi: 10.5047/eps.2009.09.002.
- [55] NERC, 'Project 2013-03 Geomagnetic Disturbance Mitigation Implementation Plan for TPL-007-1 – Transmission System Planned Performance for Geomagnetic Disturbance Events', Implementation Plan TPL-007-1, Mar. 2013. Accessed: Jun. 16, 2022. [Online]. Available: <https://www.nerc.com/pa/Stand/Pages/TPL0071RI.aspx>
- [56] X. Dong, Y. Liu, and J. G. Kappenman, 'Comparative analysis of exciting current harmonics and reactive power consumption from GIC saturated transformers', in *2001 IEEE Power Engineering Society Winter Meeting. Conference Proceedings (Cat. No.01CH37194)*, Jan. 2001, vol. 1, pp. 318–322 vol.1. doi: 10.1109/PESW.2001.917055.